

1320 Beal Avenue
Ann Arbor, MI 48109
(734) 904-1094
December 16, 2016

Michael Johnson, Airframe Lead
Nicholas Sterenberg, Avionics Lead
Michigan Aeronautical Science Association
1320 Beal Avenue
Ann Arbor, MI 48109

Subject: Final Report Transmittal for Rocket Roll Control by Use of Canards

Dear Mr. Johnson and Mr. Sterenberg:

Enclosed is our final report for the study of canards to control the roll of a rocket that Michigan Aeronautical Science Association (MASA) will fly in June of 2017 at the Spaceport America Cup competition.

The final report discusses the design and testing results of the canards and the development of the active roll control software that we are delivering to MASA. Testing was completed over the past month to adequately acquire data on the canards at several angles of attacks and wind tunnel speeds. Through our extensive design process and comprehensive testing results, we are happy to announce that the canards will sufficiently control the roll with zero angular velocity, enabling the rocket to be a major contender at the competition.

We cannot thank you enough for this exciting experience to work on such a groundbreaking project. Our team looks forward to seeing how the rocket will perform in competition and to see the useful opportunities that will arise as a result of the canard implementation. Please let us know if there is any additional work our team can do to further advance the canards. Once again, we appreciate the opportunity to help with this project and hope that this letter finds you well.

Sincerely,

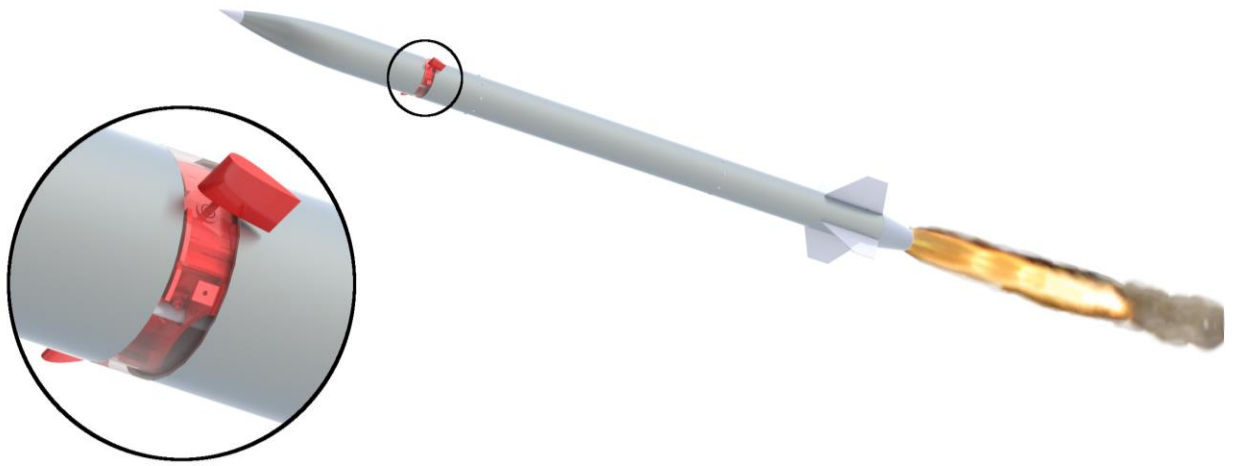
Nick Gloria

Jacob Johnson

Adam Licavoli

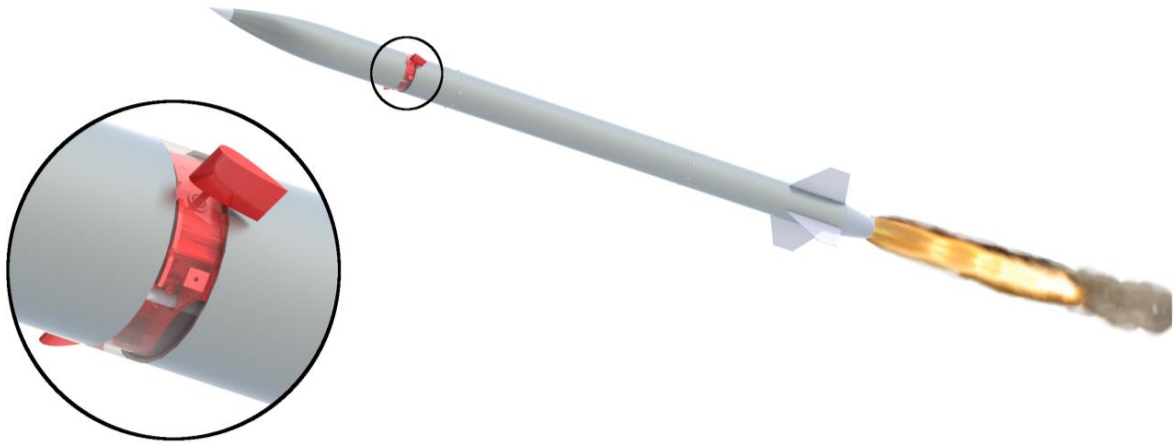
Nick Ricci

Jared Shimoun



Final Report:

MASA Rocket Active Roll Control Module



MASA Rocket Active Roll Control Module Final Report

Prepared By:

Nick Gloria
Jacob Johnson
Adam Licavoli
Nicholas Ricci
Jared Shimoun

Prepared For:

Michael Johnson, Airframe Lead
Nicholas Sterenberg, Avionics Lead
Michigan Aeronautical Science Association

Date:

December 16, 2016

Contents

Terms and Abbreviations.....	1
Executive Summary.....	2
Introduction.....	3
Results.....	5
Structure.....	5
Aerodynamics.....	8
Canard Aerodynamic Authority.....	8
Actuator Strength.....	12
Control.....	12
Sensor Package and Control Algorithms.....	12
Controller Test Results.....	14
Methods.....	15
Theory.....	16
Canard Center of Pressure using Prandtl's Lifting Line.....	16
Maximum Force on Canards.....	16
Gain Calculations.....	17
Test Setup.....	17
Apparatus.....	18
Equipment.....	19
Test Procedure.....	19
Static Test.....	20
Inertia and Friction Characterization.....	20
Dynamic Test.....	22
Uncertainty Analysis.....	22
Construction.....	23
Nose Cone.....	23
Test Stand.....	23
Canards.....	24
Costs.....	24
Schedule.....	25
Alternatives.....	26

Omissions and Limitations.....	27
Recommendations	27
Conclusion	27
References.....	28
Appendix A: Canard Sizing Simulation.....	29
Appendix B: Design Rocket Flight Profile	30
Appendix C: Roll Control Module Drawing.....	31
Appendix D: Wooden Component Schematic.....	32
Appendix F: Bill of Materials	33

Table of Figures

Figure 1: 2015 flight of MASA rocket with dynamic instability	3
Figure 2: Effect of Canards.....	4
Figure 3: Model of canard housing assembly	5
Figure 4: Exploded view of canard housing assembly.....	6
Figure 5: Assembled view of canard housing	6
Figure 6: Side View of Test Loading Experiment Setup	7
Figure 7: Canard and actuator axle schematic	9
Figure 8: Rocket overview with canard planform	9
Figure 9: Lift coefficients of a single canard over range of deflection angles and Reynolds Numbers.....	10
Figure 10: Lift curve slope as derived from fit function, with thin airfoil theory as comparison ...	11
Figure 11: Maximum lift coefficient as derived from fit function.....	11
Figure 12: Controller Overview.....	13
Figure 13: Dynamic Test 1 angular rate and roll angle error with corresponding controller commands.....	14
Figure 14: Dynamic Test 2 angular rate and roll angle error with corresponding controller commands.....	15
Figure 15: Dynamic Test 3 angular rate and roll angle error with corresponding controller commands.....	15
Figure 16: (Left) Canard planform area and calculated center of pressure and (Right) Normalized Lift distribution across canard span	16
Figure 17: 2' x 2' Wind Tunnel Schematic.....	18
Figure 18: Equipment Schematic	19
Figure 19: Top view of load balance on 2' x 2' Instructional Wind Tunnel. Airflow begins on the left of side of the figure and flows through to the right	20
Figure 20: Front View of the Spin-Up Test Setup	21
Figure 21: Spin down test results pictured left, spin up test results pictured right	22
Figure 22: Ballast and bearings on test assembly	24
Figure 23: Project Schedule	26
Figure 24: Simulated rocket roll rate for 1 degree of fin cant.....	29
Figure 25: Simulated rocket roll coefficient for 1 degree of fin cant. Note that the roll forcing coefficient represents the roll generated directly from the canards.	29
Figure 26: Mach number and Reynolds number during rocket flight.....	30
Figure 27: Schematic of Roll Control Module Assembly.....	31

Terms and Abbreviations

MASA - Michigan Aeronautical Science Association

PWM - Pulse Width Modulation

Re - Reynolds Number

C_l - roll moment coefficient

q - freestream dynamic pressure

p - freestream static pressure

T - freestream static temperature

M - freestream Mach Number

γ - ratio of specific heats

δ_{max} - maximum canard deflection angle

$S_{canards}$ - total planform area of canards

$R_{canards}$ - radius to center of pressure of canards

S_{REF} - reference area of rocket

L_{REF} - reference length of rocket

Executive Summary

MASA (Michigan Aeronautical Science Association), a student team at the University of Michigan, is developing a rocket to compete in the Spaceport America Cup. They hope to improve the rocket performance by controlling the rocket roll during flight. Previously, MASA's rocket has experienced dynamic instability where the rocket rolls and pitches rapidly in a corkscrew path, leaving the rocket short of its intended maximum altitude. This team must develop a system to minimize the rolling motion of the rocket so it can reach its maximum altitude.

MASA has asked this team to develop a roll control module to accomplish this task. Specifically, they have requested the physical hardware as an attachment to the body of the rocket, moment coefficients, and control algorithms for the module.

The optimal performance of the roll control system can be determined through simulations. Once this system is built, the moment coefficients can be obtained through wind tunnel testing. This report details our design for the roll control module and its performance characteristics that we have acquired through testing.

This group recommends that MASA accept and utilize the Roll Control Module outlined in this report. The Roll Control Module includes a set of canards, a housing unit, and the control algorithm. The module has performed to design specifications, and it has demonstrated an ability to successfully control rocket roll angle with no angular velocity or angular acceleration during wind tunnel testing. The module provided has a maximum moment coefficient of 0.23, which is expected to be sufficient to counter roll disturbances. Given the system's successful performance in a lab environment, we believe our module will successfully control the roll angle of MASA's rocket in the real world environment.

Introduction

The objective of this project is to design, build, and test a module to control and stabilize the roll rate of a rocket being developed by MASA. The stabilization of a rocket's roll presents many useful opportunities. Roll control benefits the stability of the rocket's flight as well as enabling new payload objectives. During the typical launch of a rocket, the vehicle can be driven to high roll rates, even with a mostly symmetric body. Previous MASA rockets have suffered from dynamic instability whereby the rocket would roll and pitch rapidly in a corkscrew path, leaving the rocket short of its intended maximum altitude as shown in Figure 1. While avoiding this is critical, roll stabilization also opens the door to full rocket active control. To control the rocket's trajectory actively with conventional control surfaces, the rocket must first be stabilized in roll; it is difficult to maintain a constant path while it is rapidly spinning. There are a variety of payloads that require a roll-stabilized platform. Coasting rockets present a low-gravity platform, but microgravity experiments necessitate an environment with no centripetal acceleration. Rockets with liquid propellant tanks are prone to sloshing with a rapidly rotating rocket. Cameras and instruments requiring maintenance of a specific orientation are rendered useless with high roll rates. These exciting new payload possibilities become feasible with rocket roll stability.



Figure 1: 2015 flight of MASA rocket with dynamic instability

The project will primarily impact MASA and the University of Michigan. The successful minimization of roll on MASA's rocket will greatly improve its performance in the Spaceport America Cup. This will positively affect MASA team members and expand possibilities for their future endeavors. It will also provide a pathway to further active control on MASA rockets. The implementation of a roll control system will provide a framework for additional methods of instability control in flight. It may be possible to implement a similar system on other MASA rockets, which will benefit the entire team. In addition, a victory at the Spaceport America Cup will improve the reputation of the University of Michigan. First, it will produce visible results in the form of design team achievements. Second, this type of active control has never been successfully done before at Michigan. As a result, this would be a pioneering project at the university. At the industry level, the data from this project will allow for further exploration of missile control. The project will require extensive wind tunnel testing and research into control algorithms; members of MASA who go into industry can analyze these results and apply them to other applications. The results could impact a number of future projects for sponsors.

There are several published papers that describe past work on similar control systems that are cited in the references section. Many of these control systems implement canards, which are

airfoils or flat plates that extend to affect airflow around the body of the rocket. Multiple research projects have characterized the aerodynamics of various canard shapes and forms. Hall and Landers [2] explore this exact topic by characterizing aerodynamic properties for a canard controlled missile. Other papers discuss and evaluate control algorithms implemented. This research provides a variety of algorithms that have been used. For example, Gezer and Kutay [1] explore missile roll control for an autopilot system. Further research papers such as Xin [3] and Eugene [4] discuss the idiosyncrasies of implementing a canard roll control system and the side effects on the aerodynamics of the rocket. The results of these studies have been considered during the design of MASA's roll control system.

Through analysis of this problem and previous efforts^{[1][2][3][4]}, this team has created a system to successfully control and stabilize the roll rate of the rocket using canards. By deflecting the canards, it is possible to control the roll on the rocket as shown in Figure 2. The final product for delivery to MASA is a fully functioning mechanical system that can be attached to MASA's rocket through a cylindrical insertion into the rocket airframe. There is electrical wiring to control servos that can connect directly to MASA's flight computer. The final components include canards, servos, a housing for the system, an array of moment coefficients, and suggested control algorithms. These will be delivered to MASA at the end of the Fall 2016 term.

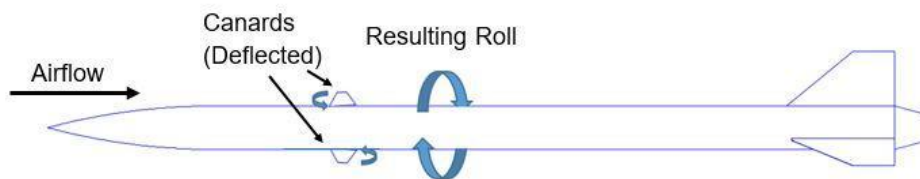


Figure 2: Effect of Canards

The design process for this system includes various levels of design and testing. First, the team researched and simulated various canard shapes and their effects on the roll of the rocket. This information was used to size the canards and determine their shape. Next, the housing was designed to accommodate and attach the canards to servos within the rocket while complying with MASA's provided constraints. After this, a test mount and a data acquisition system (DAQ) were both designed and built to allow for wind tunnel testing of the system. Finally, the moment coefficients of the roll control system were characterized through testing in the wind tunnel with the canards at various deflections with various air speeds. This report details the design process and justification behind each element of the system. It also discusses the results of testing along with recommendations.

Results

The canard module has met many design constraints and goals set forth by MASA. These consist of structural, aerodynamic, and control requirements. This section presents the outcome of the delivered product's efficacy in the context of these product requirements and goals.

Structure

The structural component of the system needs to meet criteria defined by MASA per M. Johnson personal communication on 6 Sep. 2016. These criteria give specifications for geometric constraints, strength requirements, and mass limits. The structure of the roll control system meets all the criteria provided by MASA.

The geometric constraints provided by MASA require that the system fit into a predefined volume within a 5" diameter rocket body tube. The system must be fully constrained and not allowed to rotate or translate within the rocket body. Finally, the system must be able to be assembled into a rocket body with relative ease. An elegant solution has been developed that successfully meets all of the given geometric constraints. The solution is a cylindrical module, constructed from birch plywood, which is assembled by sliding the cylinder into the rocket tube and then mounting the canards once the puck is in place. The entire housing can be laser cut and assembled very quickly allowing for design reiterations to be performed smoothly. The module is fully constrained through the use of four screws which pierce the walls of the rocket body and screw into the sides of our module radially, see Figure 3.

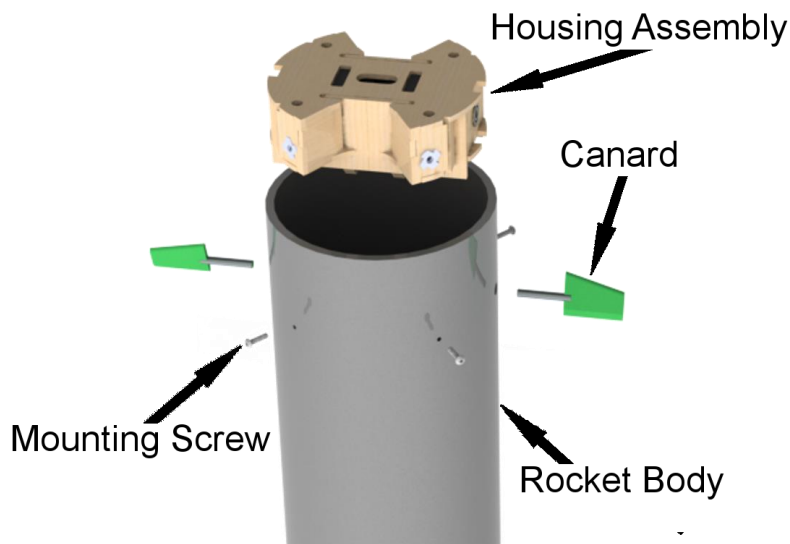


Figure 3: Model of canard housing assembly

The removable canards, servos, and top plate allow the control module to be serviced with ease even after installation.

The module itself is constructed using interlocking birch plywood panels. These panels fit together like a puzzle, as shown in Figure 4, and allow for rapid fabrication. The panels are bonded together permanently using cyanoacrylic glue with the exception of the removable top plate. Finally, carriage bolts are used to fasten the top plate to the remaining sections. Yawing and pitching moments on the canards are taken up by the four radial ball bearings. This prevents inappropriate moments from being applied to the servo. The final assembled module is shown in Figure 5.

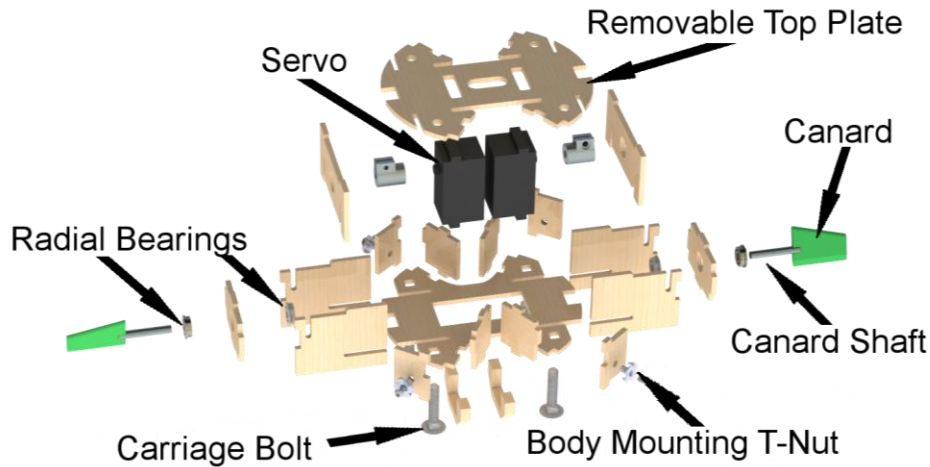


Figure 4: Exploded view of canard housing assembly



Figure 5: Assembled view of canard housing

In addition to the geometric constraints, the roll control module must be able withstand the structural stresses seen during flight. These stresses stem from both aerodynamic forces acting on the canards and 10 G launch accelerations acting on the body of the module. During launch, the point at which the rocket encounters maximum aerodynamic pressure is the point in time at which the aerodynamic forces reach their peak values. At this point in time the maximum force on the canards is projected to reach 28.6 lbs along the longitudinal axis of the rocket. The 28.6 lbs force was estimated by finding the maximum dynamic pressure in Openrocket and explained

further in the on page 16. An initial sizing of the canard shafts was done using Euler Bernoulli beam theory. The maximum stress in the canard shaft is given by Equation 1.

$$\sigma = \frac{PLr}{I}$$

Equation 1

In this equation, P is the aerodynamic force simulated as a worst case scenario at the tip of the canard, L is the length of the shaft from the tip of the canard to the servo coupling, I is the area moment of the canard shaft, σ is the maximum stress in the shaft, and r is the radius of the shaft. From this study it was determined that an aluminum shaft of 0.25 inch diameter would be able to successfully carry the aerodynamic forces from the canards to the roll control module. Equation 1 provided verification that the stresses seen in the shafts at a value of 27.2 ksi, would not exceed the yielding stress of the 6061 Aluminum at a value of 40 ksi^[6]. As such, the selected canard shaft has a safety factor of 1.47.

Physical testing was done to validate our structural design. During the test, our system has demonstrated an ability to withstand both the worst case aerodynamic loading and acceleration loading applied simultaneously. Figure 6 below shows the setup for this structural test. A weight was hung from the center of the module and sized to represent the force on the module during a 10 G acceleration. This force was scaled with an additional safety factor of 15. The system successfully survived the loading test without failure, suggesting that it would be able to structurally survive a flight.

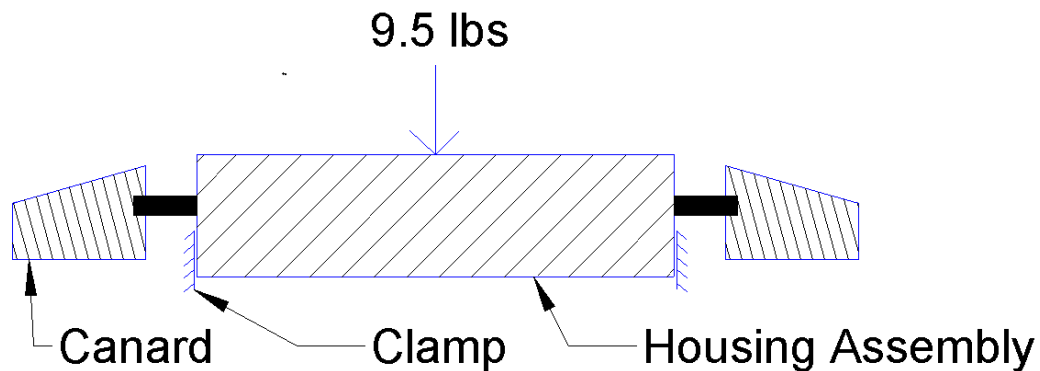


Figure 6: Side View of Test Loading Experiment Setup

As a final structural constraint, the entire module is required to fit within a 4 lbs weight budget. The roll control module meets this requirement, weighing in at 0.62 lbs.

Aerodynamics

The following sections discuss the effect of the canards on the aerodynamics of the rocket and the stability of the system.

Canard Aerodynamic Authority

In order to control the rocket's roll, the canards must be designed to provide sufficient lift and generate a roll moment that can counter disturbances. Details of the simulation discussed in this paragraph can be found in Appendix A: Canard Sizing Simulation. Past flights have demonstrated natural roll rates that reaches a maximum of approximately 2π rads/s. Videos of the launch of MASAs 10c Jim rocket and a test launch of the Massachusetts Institute of Technology's Therion rocket (both of the same scale as the design rocket) indicated maximum roll rates of approximately 1 ± 0.2 rps and 0.8 ± 0.2 rps, respectively. To size the canards, a simulation was conducted with angled fins such that a maximum roll rate of 1.6 rps was achieved, significantly greater than the test cases at about 1 rps. This corresponded to a roll moment coefficient between 0.27 and 0.3. Thus, this minimum roll coefficient was used as a benchmark.

The canards were sized to generate a moment coefficient of approximately 0.23. This is expected to be able to overcome roll induced by rocket asymmetry while avoiding unnecessarily high control power. The roll coefficient was calculated using the assumptions of thin airfoil theory for a symmetric airfoil. The roll coefficient can then be calculated using Equation 2. The canard planform is shown in Figure 7 and can be seen in the context of the rocket in Figure 8.

$$C_l = 2\pi\delta_{\max} \left(\frac{S_{\text{canards}}R_{\text{canards}}}{S_{\text{REF}}L_{\text{REF}}} \right)$$

Equation 2

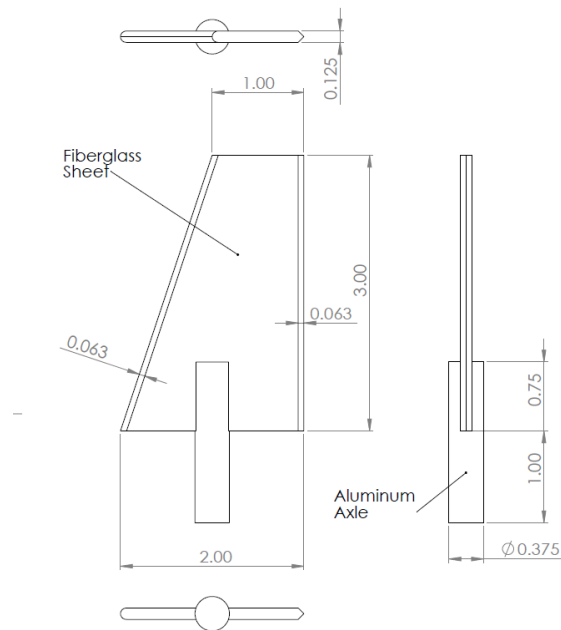


Figure 7: Canard and actuator axle schematic

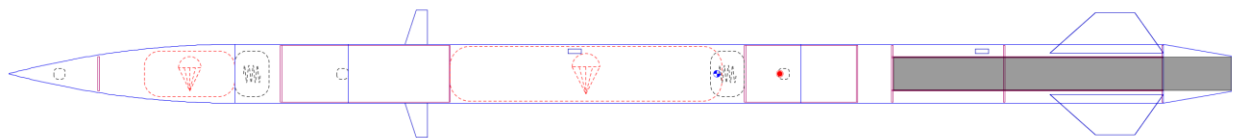


Figure 8: Rocket overview with canard planform

Testing was conducted to verify that the thin plates generated lift as expected. A static test was conducted with canard deflections acting in the same direction, generating a net side force on the test article. This side force was measured over a range of canard deflection angles and translated to a lift coefficient averaged between the two canards. Figure 9 demonstrates that the canard coefficients with respect to deflection angle can be well-characterized when fit to a function. The function chosen is shown in Equation 3 and was chosen to account for decreasing lift curve slope and stall due to separation, where $C_{L,max}$ and a_0 are the fit parameters, being the maximum lift coefficient and lift curve slope at zero deflection respectively. The function used is the error function, or the integral of a Gaussian Curve.

$$C_L = C_{L,max} * \operatorname{erf}\left(\frac{a_0\sqrt{\pi}\delta}{2C_{L,max}}\right)$$

Equation 3

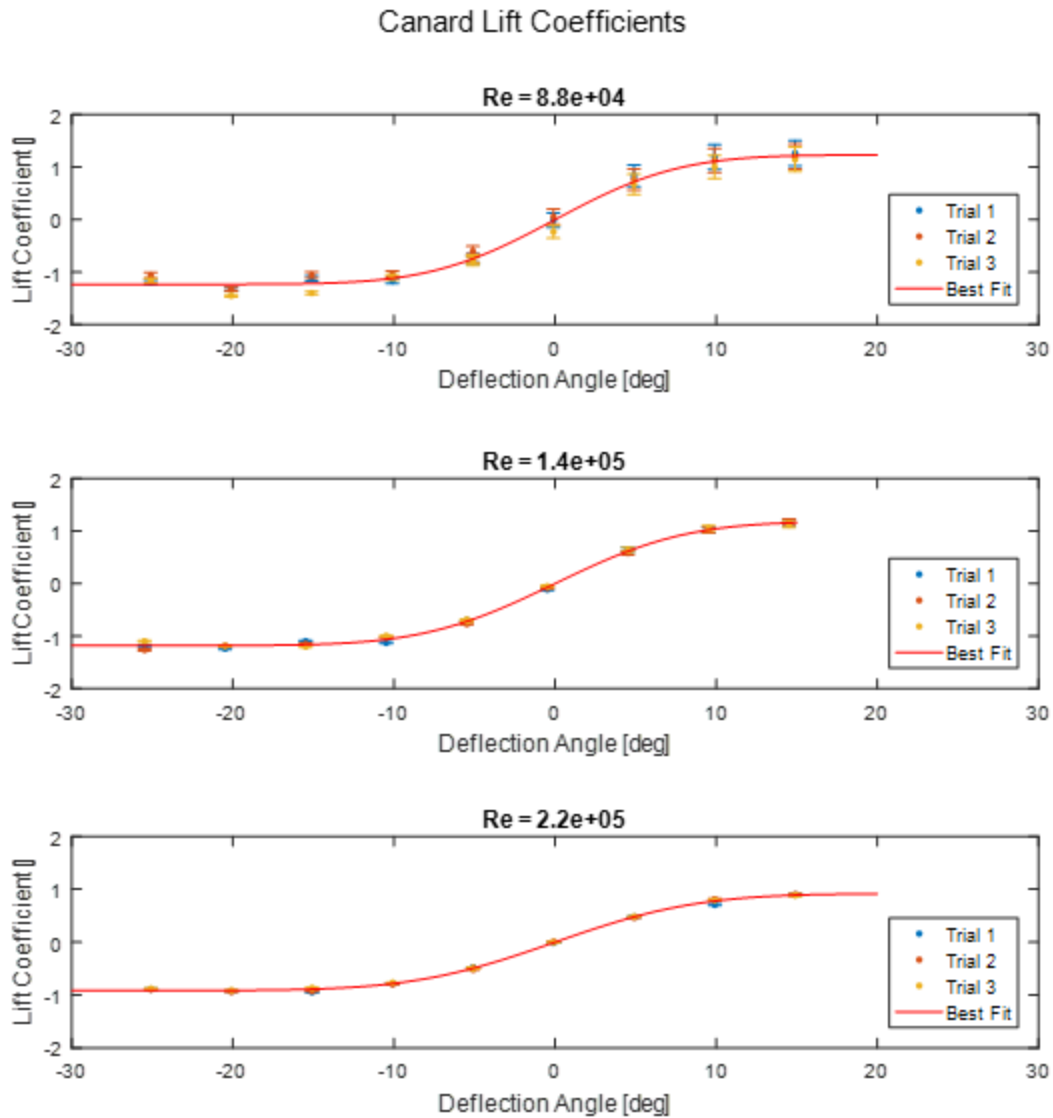


Figure 9: Lift coefficients of a single canard over range of deflection angles and Reynolds Numbers

This data is plotted against Reynolds Number for the rocket, based on a reference length of the rocket diameter. It is important to note that the rocket will experience a Reynolds number between 0 and 50,000,000 during flight and that this data was collected at a maximum Reynolds number of 220,000. The data was processed by defining a deflection angle of zero such that no net lift was generated. Details on the uncertainty analysis used for the error of the lift coefficient points can be found in the Test Procedure section.

The fit parameters, being the maximum lift (or roll) coefficients and the slope of the lift curve a_0 , are shown in Figure 10 and Figure 11 respectively. Error bars were generated using a 95% confidence interval of the fit parameters.

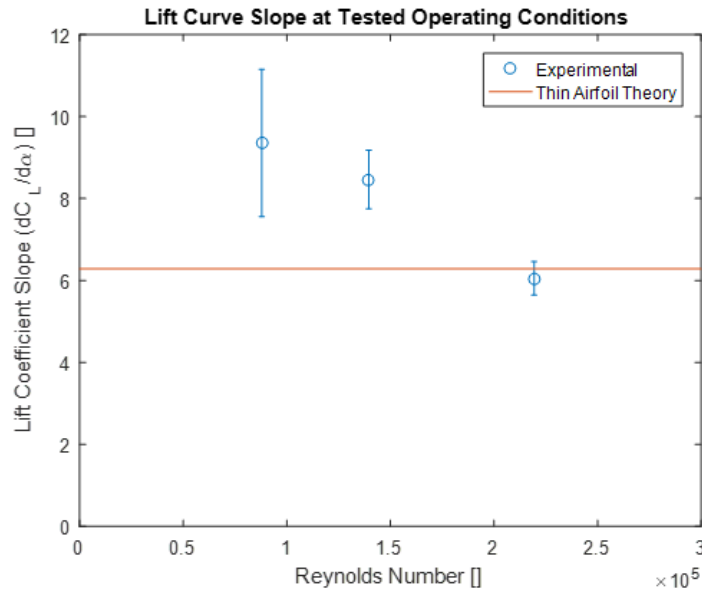


Figure 10: Lift curve slope as derived from fit function, with thin airfoil theory as comparison

The lift curve slope was expected to be approximately the same as a thin airfoil considering that the design is a flat plate with rounded leading edges and a chamfered trailing edge. However, thin airfoil theory would not account for the presence of a curved rod at approximately half of the chord and protruding one quarter of the span. The experimental data show that the lift curve slope is in approximately the right range as expected.

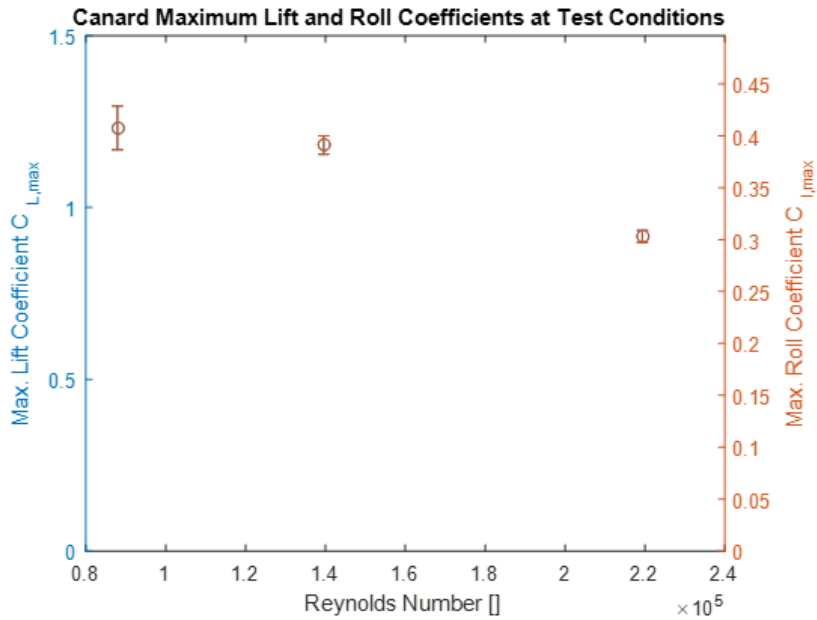


Figure 11: Maximum lift coefficient as derived from fit function

The maximum roll coefficients can be found using Equation 4. The canard moment arm, R_{canard} , is the distance of the canard center of pressure from the rocket centerline and is 4.06" (1.460" from rocket body), as explained on page 16 using Prandtl's Lifting Line theory for finite lifting surfaces.

$$C_l = C_{L,max} \left(\frac{S_{canards} R_{canards}}{S_{REF} L_{REF}} \right)$$

Equation 4

It is clear from the data that a maximum roll coefficient between 0.3 and 0.4 was demonstrated. This exceeds the goal roll coefficient of 0.2 to 0.3 required to overcome expected rocket roll due to perturbations and rocket asymmetry. Therefore, the canard design has a roll authority that exceeds the expected demand.

Actuator Strength

The actuator strength requirement was set by the operating condition at maximum dynamic pressure and maximum canard deflection (10°). The maximum canard lift force was found as 28.3 lbf and the center of pressure was found to be 0.865" behind the root chord leading edge in the axial direction (see the calculation from Prandtl's Lifting Line theory on page 16).

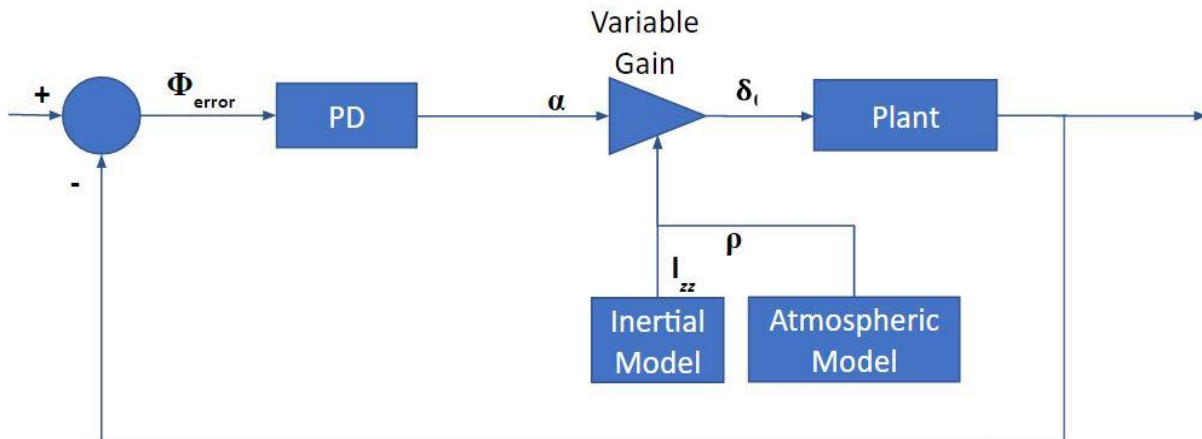
Considering that the actuator axis is 1" from the leading edge, the moment arm is thus 0.135". This results in a maximum moment on the canards of 3.82 lbf-in. Since the servo is capable of 4.77 lbf-in torque, the servo has sufficient strength by a factor of 1.25.

Control

The roll control system electronics must meet all of the requirements provided by MASA. Primarily, the control algorithm should integrate with MASA's electronics and it must successfully minimize the roll rate of the rocket. The following section discusses the structure of the control algorithm and the results of dynamic testing.

Sensor Package and Control Algorithms

To successfully stabilize the rocket, the roll control module must be compatible with the sensor package and flight computer provided by MASA. Specifically, the system must be able to produce a realistic deflection angle based on the given inputs into the system from the sensors that complies with the servo deflection limit and prevents stall. The control algorithms have been delivered along with the module to accomplish this task. The algorithm accepts a roll angle error as the input. This can be obtained from the sensor package which includes 3 axes of accelerometer, magnetometer, and gyro data. In this team's particular implementation, the roll angle was determined using the arctangent of the accelerometer readings in the x and y axes. The full control algorithm is shown in Figure 12 below where the plant is the canards.



Φ_{error} = roll angle error
 α = requested roll angle
 δ = requested canard deflection
 ρ = density of atmosphere
 I_{zz} = Moment of inertia (z axis)

Figure 12: Controller Overview

The algorithm sends the roll angle error through a PD (Proportional and Derivative) controller. The requested angles are subjected to variable gains shown in Table 1 below. These gains convert from a roll angle error and a roll rate error, to canard deflections and thus have units of seconds and seconds² respectively. Factored into the gains is the velocity, canard characterization, atmospheric density, Mach number, and the roll moment of inertia of the rocket. As such these gains can be recalculated during flight to account for changes in velocity, Inertia, Mach number, and air density.

Table 1: Controller Gains

Controller	Gain
Proportional	0.83 s
Derivative	-1.03 s ²

The gains were determined using the process shown in the Theory section under Methods. After applying gains, the resulting values from each controller are added together to create a requested deflection for the canards. These deflections are sent to the servos subject to a maximum and minimum deflection of positive and negative 10 degrees to prevent stall.

This algorithm can be easily integrated into the MASA flight computer. Using the sensor inputs, it is possible to implement the control algorithm through basic C code on their BeagleBone

Black. This team used the Arduino IDE (Integrated Development Environment) along with a Teensy 3.6 for initial testing. However, the Arduino IDE is C-based so it can be effortlessly ported to the BeagleBone Black. Thus, it is possible to add all necessary elements of the roll control module to MASA's avionics system.

Controller Test Results

The control system was tested in the wind tunnel through dynamic testing as described in the Methods section below. The objective was to prove that the control system could successfully achieve close to a desired target roll angle with a minimal roll rate at equilibrium. The controller succeeded in this task.

During dynamic testing, the target roll angle was set to automatically change at 30 second increments. This would provide a disturbance to the system and test its ability to deal with the results of this disturbance. At the moment the target angle changes, the controller sends a deflection to the canards to adjust the system to this new target angle. The controller changes these deflections based on the algorithm until the system has reached the target angle with zero roll rate. While in use on a rocket, the system should reach equilibrium at the target angle. However, the following plots show that the proportional controller is still active once the system reaches equilibrium and there is some roll angle error. This is the consequence of a constant moment from the fins on the test apparatus described in Test Setup below. Because of this variation, the system can be deemed successful if the roll angle is constant and the roll rate is zero. The results of the first dynamic test are shown in Figure 13 below.

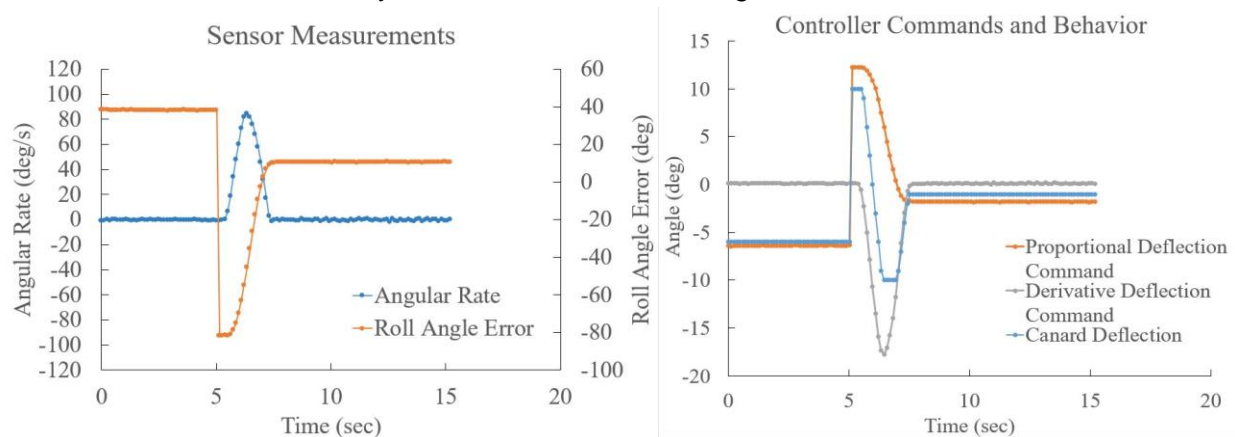


Figure 13: Dynamic Test 1 angular rate and roll angle error with corresponding controller commands

In the above test, the target roll angle switches at Time = 5 seconds. The system takes approximately 2.5 seconds to return to equilibrium at a new roll angle with zero roll rate. Another successful test is shown in Figure 14 below.

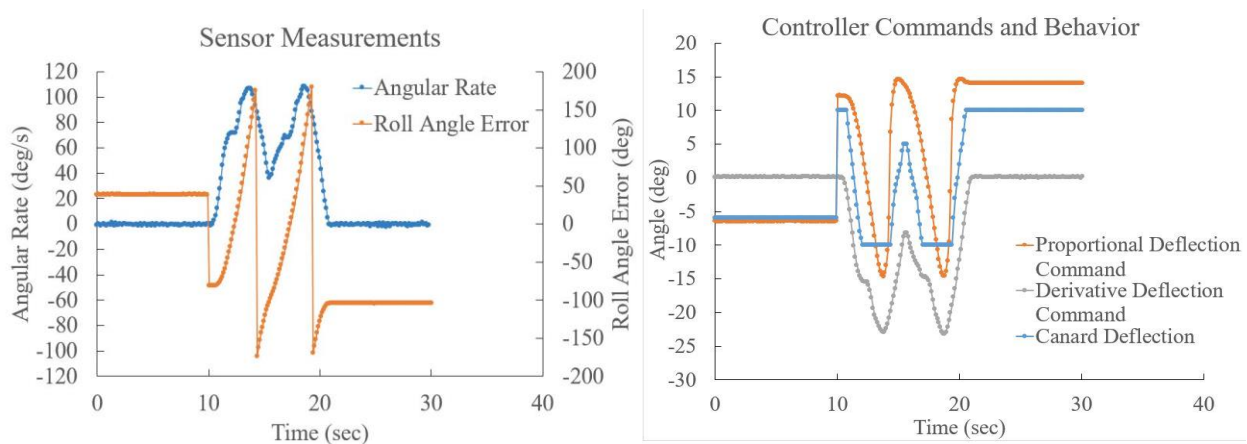


Figure 14: Dynamic Test 2 angular rate and roll angle error with corresponding controller commands

In this test, the target roll angle switches at Time = 10 seconds. This target angle was slightly more difficult to achieve so it took approximately 20 seconds to reach equilibrium. However, it is still able to achieve zero roll rate. The final dynamic test is shown in Figure 15 below.

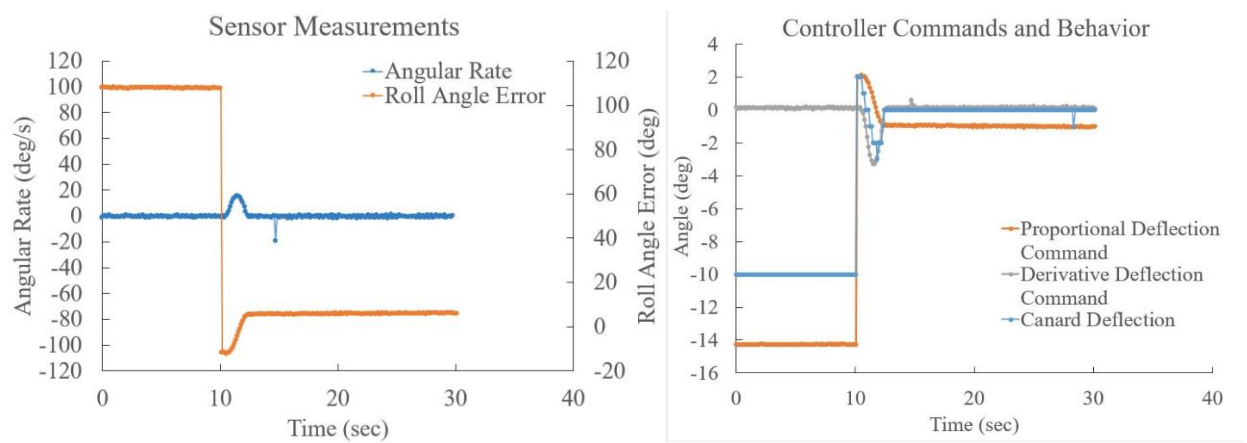


Figure 15: Dynamic Test 3 angular rate and roll angle error with corresponding controller commands

In the last test, the target roll angle switches at Time = 10 seconds. It takes the system approximately 2.5 seconds to return to zero roll rate at equilibrium. These the tests show the successful performance of the roll rate control system in achieving its goals.

Methods

The following sections discuss the methods for the design, construction, and testing of the physical components of the roll control system.

Theory

This section discusses the theory underlying some of the design-related assertions in this report.

Canard Center of Pressure using Prandtl's Lifting Line

In order to determine the maximum torque on the canard actuator axis, Prandtl's lifting line theory was used to generate a lift distribution across the canard. This theory accounts for vortex shedding along the lifting surface and the resulting redistribution of lift.

With an analysis conducted at 10° deflection of the canard, the maximum allowed deflection, the lift distribution and center of pressure was found. Figure 16 shows the results of this analysis. The center of pressure is approximately at the quarter-chord line at about half-span. The exact coordinates are 0.865" behind the root chord leading edge and at 1.460" in semispan.

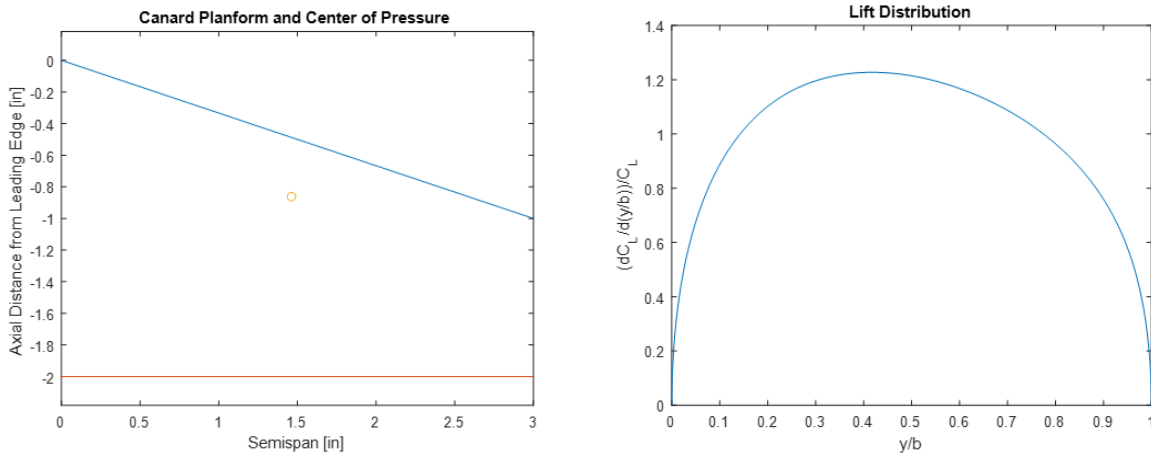


Figure 16: (Left) Canard planform area and calculated center of pressure and (Right) Normalized Lift distribution across canard span

Maximum Force on Canards

In OpenRocket, the dynamic pressure, q , was found by Equation 5 at a Mach number of .7. This Mach number was used because it is the maximum Mach operating condition to avoid strong transonic effects. Assuming a maximum angle of attack of 10°, the coefficient of lift was determined using thin airfoil theory as seen in Equation 6. A correction in the coefficient of lift for compressible flow was applied with Equation 7. Applying all of these equations together, the total lift was found to be 28.3 lbf from Equation 8.

$$q = \frac{1}{2} \gamma p_{\infty} M_{\infty}^2$$

Equation 5

$$C_{L,incompressible} = 2\pi\alpha$$

Equation 6

$$C_L = \frac{C_{L,incompressible}}{\sqrt{1 - M_{\infty}^2}}$$

Equation 7

$$L = qSC_L$$

Equation 8

Gain Calculations

The controller gains were determined experimentally during testing and converted using Equation 9 listed below. q is the dynamic pressure during dynamic testing. S is the area of the canard, r is the radial distance from the longitudinal axis of the rocket to the center of pressure of the canard, $\frac{dC_L}{d\alpha}$ is the change in lift coefficient due to angle of attack as determined in static testing, C is the gain value determined from testing each controller and used in the proposed control algorithm, I is the moment of inertia of the test rocket as determined experimentally. Finally, K is a gain in units of angular acceleration per unit of error or error time rate of change. This gain can be universally applied to other system with different inertia or canard designs.

$$K = C \left(\frac{qS_{canards}R_{canards} \frac{dC_L}{d\alpha}}{I} \right)$$

Equation 9

Test Setup

Although the canard roll control system will eventually be tested onboard a transonic sounding rocket, this project seeks to test and validate the roll control system in a wind tunnel setting. Loss of control or instability during a test launch could lead to a failed launch and damage to equipment. This testing seeks to drastically reduce the risk associated with the first test launch.

First, a static test provided an understanding of moment coefficients due to changes in the angle of attack of the canards. The test article was placed in the wind tunnel under static conditions. With the wind tunnel powered on, the angle of attack of the canards was cycled through -20° to 20° . This process was repeated numerous times under increasing wind speed in order to gain an understanding of behavior changes due to increasing Reynolds Numbers. By analyzing the forces picked up by the force transducers on the wind tunnel the moments on the simulated rocket were determined.

Next, a characterization of the test apparatus was performed to quantify the inertia and friction in the system. The test article was spun up and then slowly allowed to decelerate due to parasitic friction in the system. In a separate test, a known moment was applied to the system at rest causing spin. In both tests the rate of rotation was directly observed.

Lastly, a dynamic test provided an understanding of how the control system would react under more realistic conditions. In this instance, the test article was allowed only rotational movement on the longitudinal axis of the rocket. The behavior of the canards due to the rotation was directly observed.

Apparatus

A wind tunnel was required for this testing in order to collect data on the test article in a controlled environment. The University of Michigan's Subsonic 2 ft x 2 ft Instructional Wind Tunnel, as depicted in Figure 17, was chosen for use with this project. This tunnel is the best available tool to simulate the rocket in flight. The simulated airframe at full-scale has a diameter of five inches. The cross sectional area of the test article is 3.4% of the wind tunnel flow area, allowing accurate simulation of the aerodynamics.

The wind tunnel can also simulate the flight of the rocket in all of the incompressible regime of airflow. While the rocket will experience Mach numbers up to 0.8 during flight, a major part of the flight is within the incompressible regime.

The wind tunnel has a test section area of 2' by 2' and can simulate velocities up to about 30 m/s. It has a sensor for dynamic pressure, used to determine the freestream velocity, and load transducers to measure aerodynamic forces.

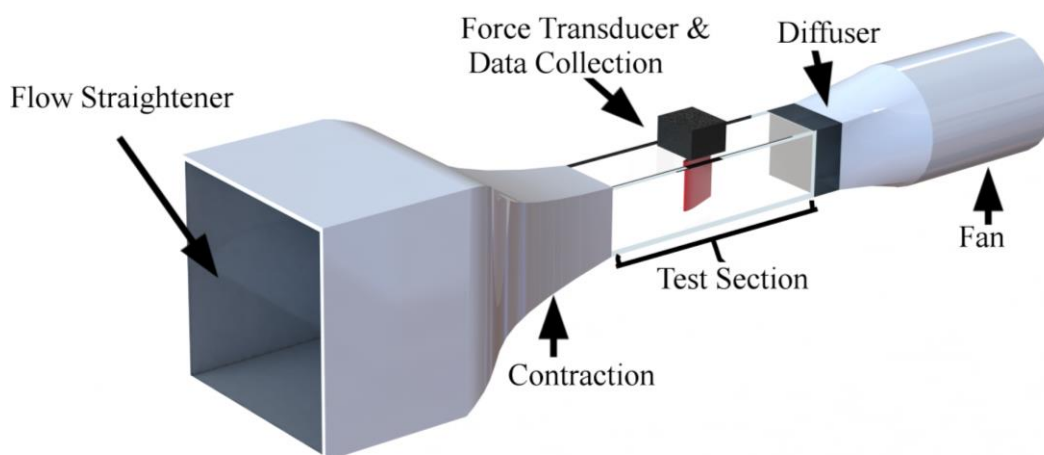


Figure 17: 2' x 2' Wind Tunnel Schematic

Equipment

In order to effectively test a free-spinning rocket in a wind tunnel, a special mounting apparatus has been created, shown in Figure 18. This mounting apparatus was suspended from a mount on the ceiling of the wind tunnel. The simulated airframe was attached from the rear by a rod in line with its axis of symmetry. This rod was supported by two mounted bearings and attached to the mounting frame. Furthermore, a ballast was placed on the aft end of the rod on the other side of the bearing such that the center of mass of the entire apparatus was directly in line with the supporting beam. Additionally, the ballast was constructed in such a way to simulate the moment of inertia expected from the full sized rocket.

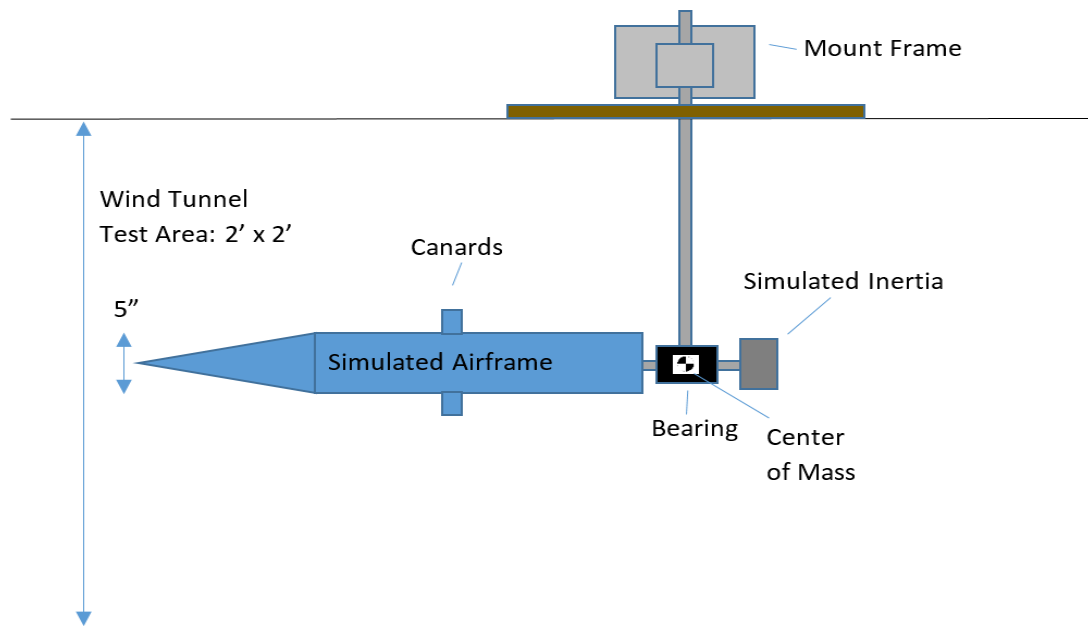


Figure 18: Equipment Schematic

In order to test no-spin conditions, the rod can be clamped in position, allowing no rotation. Both static and dynamic tests will use the same test apparatus with only minor variations as described below.

Test Procedure

The following sections discuss the static, inertial, and dynamic testing of the canards, as well as the characterization of the testing apparatus.

Static Test

In this test the rocket is not allowed to move in any way. The first part of this experiment is to calibrate the force transducers by loading them with some known weight and measuring the voltages produced. The force balance orientation is described in Figure 19.

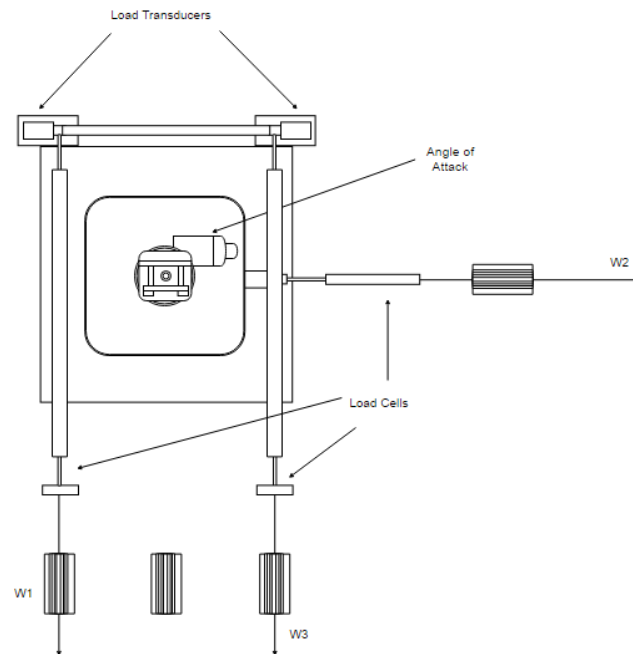


Figure 19: Top view of load balance on 2' x 2' Instructional Wind Tunnel. Airflow begins on the left of side of the figure and flows through to the right

There are three load cells in this setup. Load cells W1 and W3 measured the lift force applied on the rocket. W2 measured the drag on the rocket. The test article is oriented in the wind tunnel such that the lift forces from the canards act horizontally on the rocket. From there the wind tunnel was set to desired speeds while the canards were deflected in the same direction by a specific angle of attack. Each angle will produce a distinct force on the test stand and which will be read by the force transducers. Three wind speeds were tested with three trials at each setting.

Inertia and Friction Characterization

For this test, the simulated airframe and mounting apparatus were placed outside of the wind tunnel. The onboard data acquisition system was switched on and set to record accelerometer values perpendicular to the axis of rotation. The simulated airframe was then spun up by hand to around one rotation per second and its spin was allowed to slowly decay. This procedure was repeated twice.

In a separate test, a moment was applied to the simulated airframe as shown in Figure 20 below.

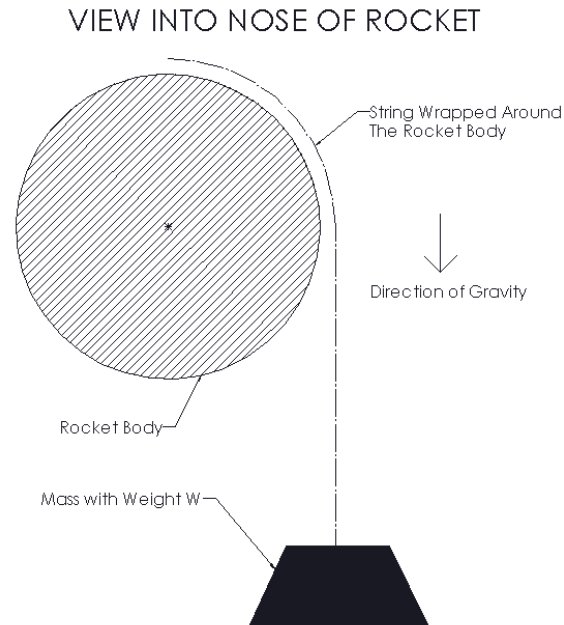


Figure 20: Front View of the Spin-Up Test Setup

The test apparatus was held at rest initially and then released. The onboard data acquisition system was set to record accelerometer values as before. The accelerometer data was then reduced to roll rates using Equation 10.

$$\ddot{\phi} = \frac{d}{dt} \arg(a_y + a_z i)$$

Equation 10

Fitting a line to both the spin-up and spin-down tests allowed us to find the angular acceleration in both tests. A derivation of rotational dynamics yields Equation 11 and Equation 12.

$$I_{zz} = \frac{M_{fric}}{\alpha_{spin\ down}}$$

Equation 11

$$I_{zz} = \frac{mgr + M_{fric}}{a_{spin\ up}} - mr^2$$

Equation 12

In these equations, I_{zz} is the inertia of the system about its axis of rotation, M_{fric} is the moment on the system due to friction, m is the weight of the falling mass, g is the acceleration due to gravity, and r is the radius of the rocket tube, $a_{spin\ down}$ is the measured rate of angular deceleration from the spin down test, and $a_{spin\ up}$ is the measured rate of angular acceleration from the spin-up test. Solving Equation 11 and Equation 12 gave the inertia and friction in our test rig. The angular velocity profiles of sample test trials are shown in Figure 21. The friction was determined to be a steady 0.29 ft-lbs and the inertia as 0.059 slug-ft².

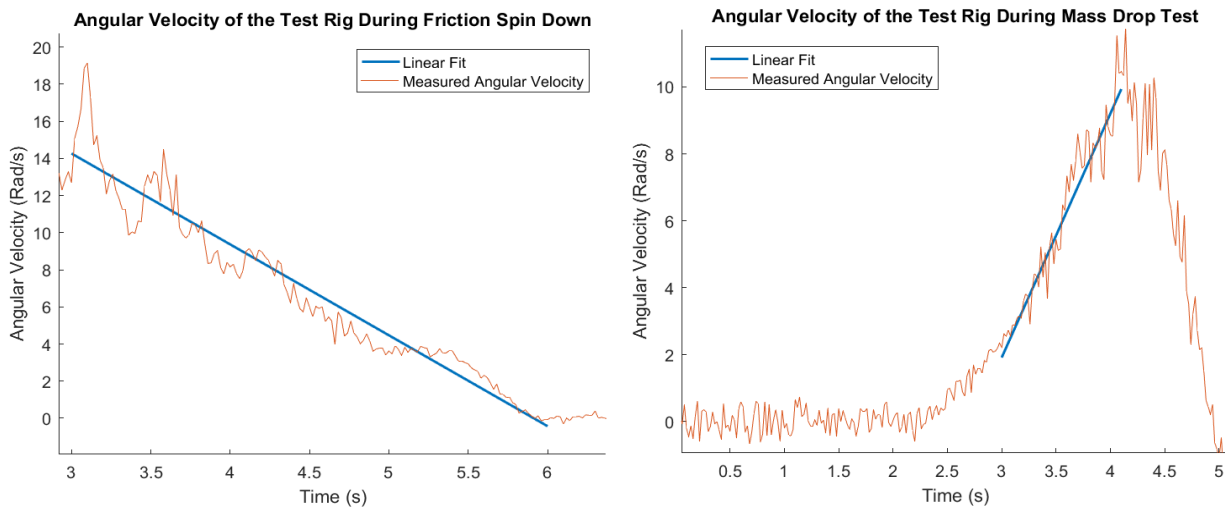


Figure 21: Spin down test results pictured left, spin up test results pictured right

Dynamic Test

For the final test the rocket is allowed to rotate about its roll axis only. No other movement is allowed. In order to force a rotation on the test article and to simulate a constant moment during testing additional fins were included with this test. The fins were flat metal plates bent at a 45° relative to the air flow and connected to the ballast. The wind tunnel was set to the desired speed and the test article was allowed to begin rotating. Once rotations had begun the controller was turned on and active control began. The behavior of the system could then be observed in person while information regarding rotational rates and time were taken by the sensor suite onboard the test article.

Uncertainty Analysis

Uncertainty was accounted for in the coefficient testing with the following equations. Here, F represents a generic load, and V_1 through V_3 represent the three load cell output voltages.

$$\Delta q = q \left(\left(\frac{\Delta p}{p} \right)^2 + \left(\frac{\Delta T}{T} \right)^2 \right)^{0.5}$$

Equation 13

$$\Delta F = F \left(\left(\frac{\Delta V_1}{V_1} \right)^2 + \left(\frac{\Delta V_2}{V_2} \right)^2 + \left(\frac{\Delta V_3}{V_3} \right)^2 \right)^{0.5}$$

Equation 14

$$\Delta C_l = C_l \left(\left(\frac{\Delta F}{F} \right)^2 + \left(\frac{\Delta q}{q} \right)^2 \right)^{0.5}$$

Equation 15

Construction

Four major parts were required to be designed for the experiments. The nose cone, the servo housing, the test stand, and the canards. The servo housing has already been discussed so this section will focus on the remaining three components. A portion of the body of the rocket made out of fiberglass has been provided by MASA and serves to couple most of the system together.

Nose Cone

The nose cone was made out of foam and was constructed with the use of a CNC router. The router was used to cut several layers of increasingly smaller circular pieces of foam which were then secured together and the rough sections filled in with spackle. The shape of the nose cone was determined by MASA.

Test Stand

The test stand is constructed using a combination of steel, aluminum, wood, and foam. First the simulated inertia ballast was constructed using a 12" strut channel and stock steel cut to two 2.5" square pieces with a weight of 2.25 lbs each. The stock was then secured to either end of the channel at a radius of 5 1/2" to produce the desired moment of inertia of 0.05 kg-m² or 0.037 slugs-ft². The ballast and most of the stand assembly can be seen in Figure 22 below.

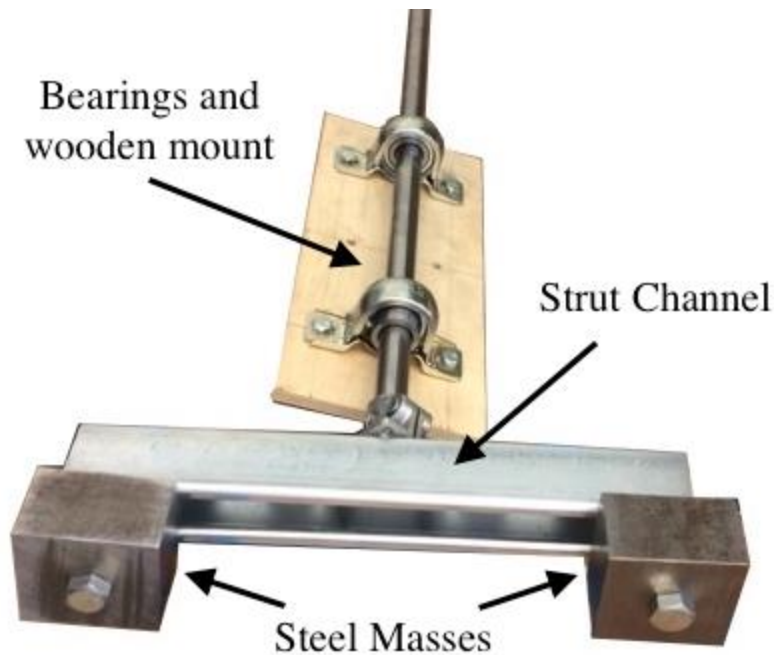


Figure 22: Ballast and bearings on test assembly

The ballast was then secured to one end of a steel shaft that runs through two mounted ball bearings and ends with two circular pieces of foam secured to the shaft. The ball bearings, shaft, and clamp are all $\frac{3}{4}$ " diameter with the bearings secured to a 12" x 4" wooden board. The two foam pieces served to both secure the sensor suite between them and insert snugly into the rocket frame in order to translate the rotation of the rocket to the shaft. All of this was supported by an aluminum rod clamped on one end to the wooden board and to the wind tunnel on the other.

Canards

The canards are small pieces of $\frac{1}{8}$ " thick fiberglass cut out using a bandsaw. Once they had been cut the pieces of fiberglass were placed onto a belt grinder to have their leading edges rounded and trailing edges tapered to a point. The canards were then epoxied into a slit cut out of a thin aluminum rod with a diameter of $\frac{1}{4}$ ", which was in turn coupled to the servos.

Costs

The total cost for the completed project is \$31,300. Table 2 shows the cost breakdown of the project. The majority of the cost comes from the labor put into the project. Engineers were billed out at \$35 per hour for a total of 600 hours. The next highest cost comes from the facilities. There have been 4 complete days in both the wind tunnel and the machine shop which cost \$150 and \$80 per day respectively. The smallest portion of the budget comes from the

materials. Between the canards, test frame and housing, all of the materials will cost \$368. The budget also includes a 40% overhead.

In the proposal stage we underestimated the amount of hours that our engineers would spend on the project. It was originally estimated that the engineers would spend 320 hours on the project; however, the engineers billed out a total of 600 hours. This change in hours caused the labor budget to increase substantially. Also, there was an incorrect estimation on the cost of materials. The final materials cost was \$300 less than estimated.

Table 2: Final Project Budget

Category	Item	Unit Cost (\$)	Units	Cost
Labor	Engineer	35/hr.	600	21000
	Machinist	30/hr.	5	150
	Subtotal			21150
Facilities	Shop	80/day	4	320
	Wind Tunnel	125/day	4	500
	Subtotal			820
Materials	Canards	-	-	\$64.81
	Test Frame	-	-	\$180.81
	Housing	-	-	\$141.16
	Subtotal			\$386.78
Total				\$22,356.78
Overhead			40% of Total	\$8,942.71
Grand Total				\$31,299.49

Schedule

There were many moving pieces in this project that determined its schedule. The big milestones for this project was the coefficient test and the free roll test. The first phase of testing, which was the coefficient test, was completed on November 20th and the final free roll test was completed on December 4th. The final project was completed by December 8th. The final Gantt chart can be seen below in Figure 23.

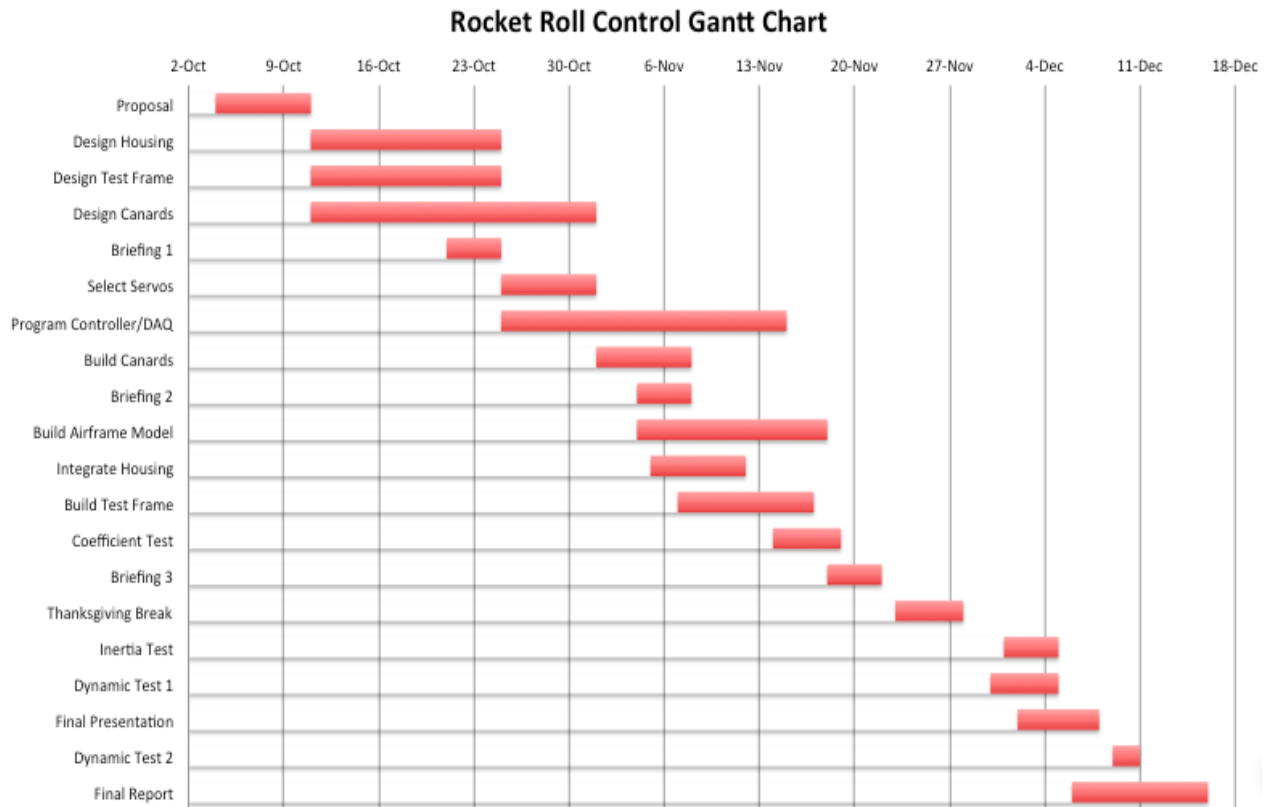


Figure 23: Project Schedule

Alternatives

There are potential alternatives to the canard-based roll control module proposed above. However, most of these would require extensive design and testing, which would be costly. If the proposed module is not satisfactory, the simplest alternative is to use the same housing and actuators but with different canards. For example, MASA can remove the flat plate canards and replace them with airfoil-shaped canards. They can also use different sized canards if it would better suit their needs.

A costlier alternative is an entirely new module. With a new module, it is also possible to implement fins rather than canards. Fins would be placed further towards the bottom of the rocket and are generally much larger. However, this change in position would affect the avionics. One major reason why canards were used initially is that it is much easier to integrate with MASA's avionics because of the canard location relative to the avionics bay. MASA would need to think of a different way to connect fins to their avionics if they choose to use this alternative.

Omissions and Limitations

There were several design omissions and limitations. For starters, we were unable to test the roll control system under real conditions in a real test launch due to time constraints and lack of a testing location. Since the rocket roll system was only tested in the wind tunnel, it was not tested at the maximum Reynolds number that it will see during flight. Also, the roll system was not integrated into the entire rocket due to the size constraints of the wind tunnel and only integrated into a test section. Although we are confident that the roll control system will work well, we did not test how the canards will affect the aerodynamics of the rocket that is behind the canards.

Another strong limitation in our testing was the test setup and apparatus. The apparatus that we used had high friction in the bearings. The friction in the bearings had to be overcome by the forces applied by the wind tunnel. This friction required us to increase the wind tunnel speed close to its maximum speed in the dynamic testing.

Recommendations

There are additional ways to improve the roll control system. The most significant area that MASA should investigate is improvement to the controller. The roll control team was able to test a small range of gains and controller configurations but there are additional possibilities that could be more effective.

It would also be worthwhile to consider improvements on the canard design. While the flat plate used by this team was proven to work the performance would likely be improved by providing an airfoil shape and removing the blunt leading edge. Specifically, increasing the stall angle of the canard would go a long way to improving the robustness of the roll control system.

Additional testing using the supersonic wind tunnels available to University of Michigan may also be prudent to better characterize the behavior of any canards proposed in the future with the high Reynolds numbers they are likely to see in flight.

Conclusion

The final roll control system meets all structural and geometric criteria given to us by MASA. The aerodynamics roll coefficients of the canards not only meet our prediction, but are large enough to control the roll of the rocket during launch. The final price tag for the complete project comes in at \$33,500. The majority of this cost comes from the extensive engineering labor over the past few months. The project was completed on schedule and presented in poster form on December 8th, 2016.

References

- [1] Gezer, R. Burk and Ali Turker Kutay. "Robust model following control design for missile roll autopilot." *Control, 2014 UKACC International Conference*, 2014
- [2] Hall, Les and Michael Landers. "Aerodynamic Predictions of Pitch and Roll Control for Canard-Controlled Missile." *AIAA Paper 2000-4516*, 2000
- [3] Jianren, Xin, Xie Kan, and Lieu Yu. "Controlled canard configuration study for a solid rocket motor based unmanned air vehicle." *Journal of Mechanical Science and Technology*, 2009
- [4] Tu, Eugene. "Effect of Canard Deflection on Close-Coupled Canard-Wing-Body Aerodynamics." *AIAA Paper 92-2602*, 1994
- [5] Marks, Lionel S., Theodore Baumeister, Eugene A. Avallone, and Theodore Baumeister. *Marks' standard handbook for mechanical engineers*. New York: McGraw-Hill, 1978. Print.

Appendix A: Canard Sizing Simulation

A simulation was conducted using OpenRocket with MASA's 10,000 ft sounding rocket design. Fin cant or angled fins of 1 degree was used to generate a roll coefficient simulating roll from rocket asymmetry.

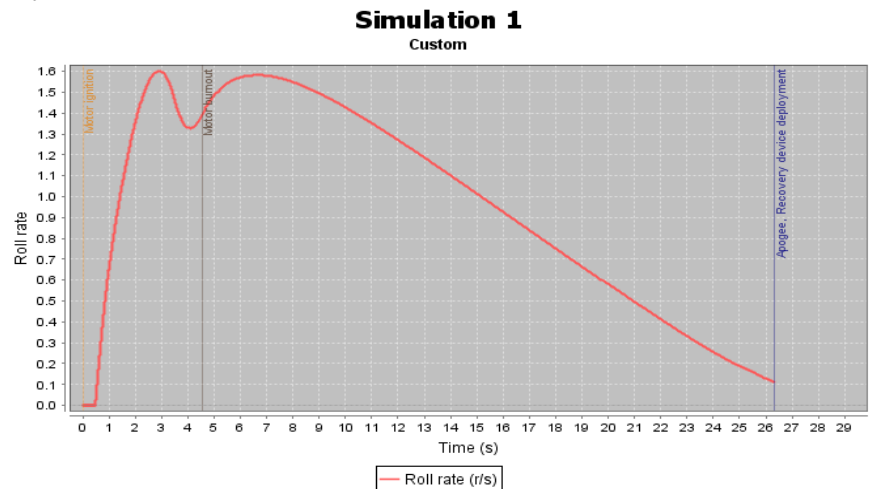


Figure 24: Simulated rocket roll rate for 1 degree of fin cant

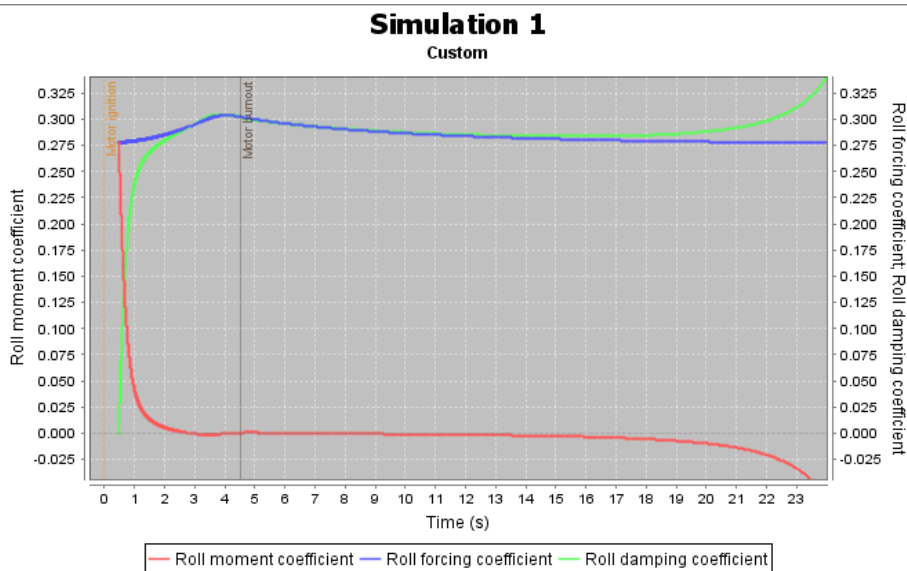


Figure 25: Simulated rocket roll coefficient for 1 degree of fin cant. Note that the roll forcing coefficient represents the roll generated directly from the canards.

It can be concluded from this study that a roll coefficient of 0.3 corresponds roughly to a maximum roll rate of 1.6 Hz.

Appendix B: Design Rocket Flight Profile

This section provides background on the rocket with which the rocket will be used and its expected flight. The simulation software OpenRocket was used to generate this data.

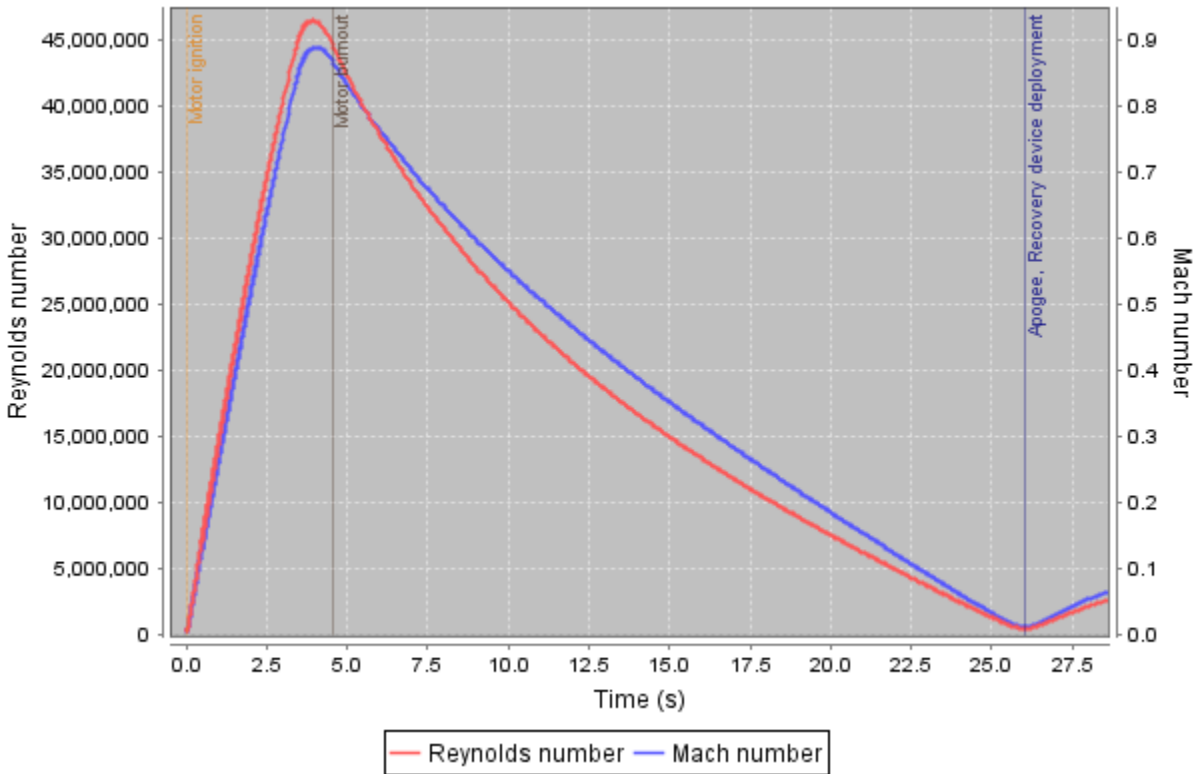


Figure 26: Mach number and Reynolds number during rocket flight

Appendix C: Roll Control Module Drawing

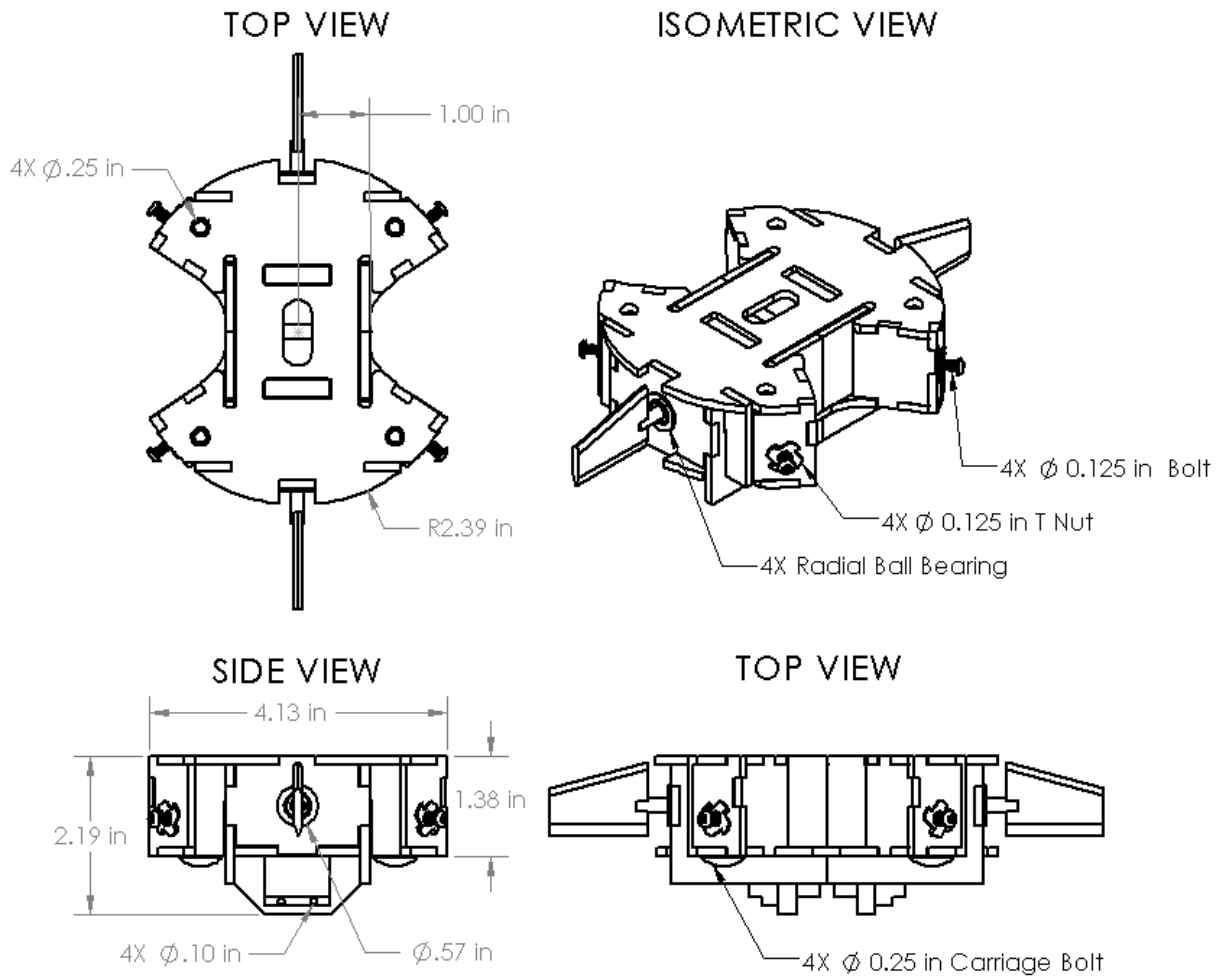
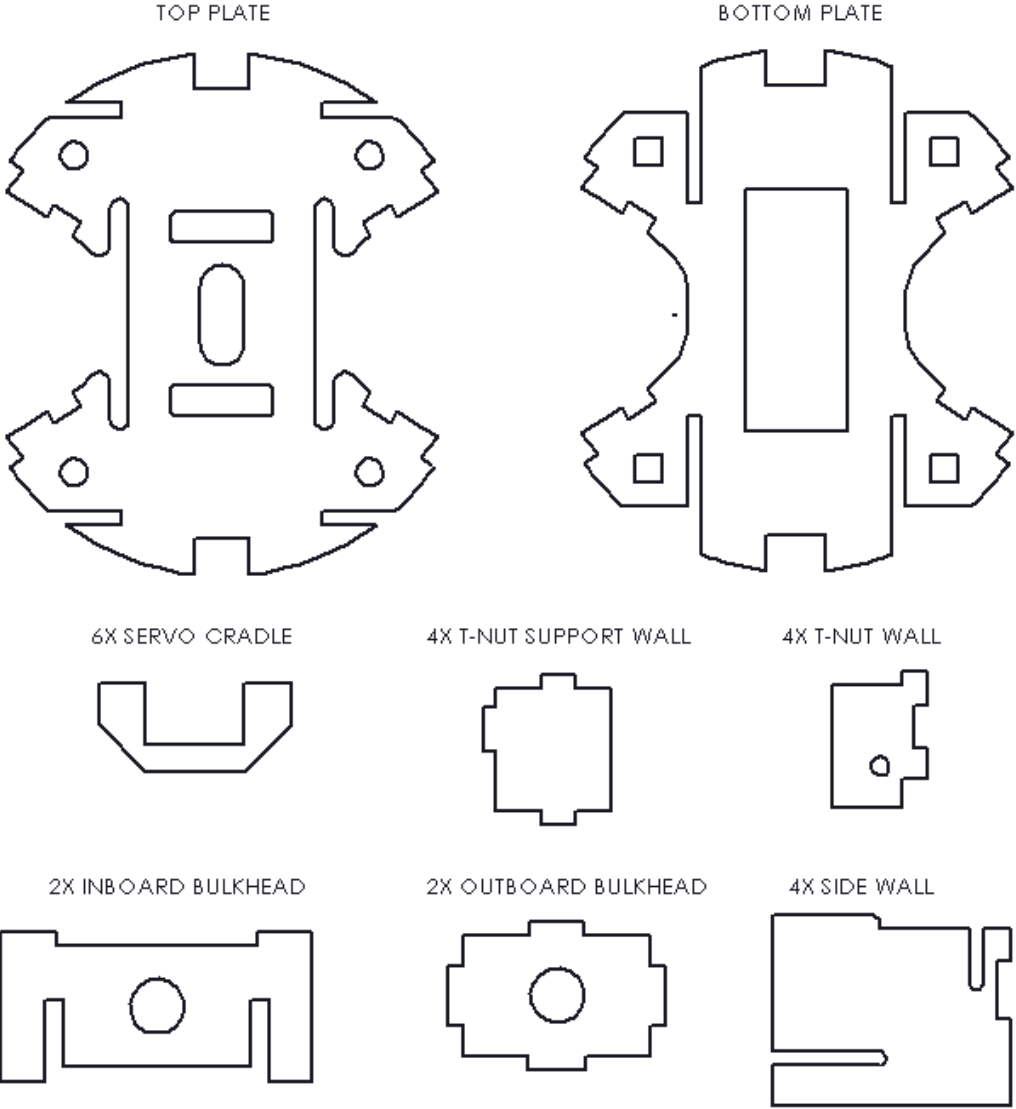


Figure 27: Schematic of Roll Control Module Assembly

Appendix D: Wooden Component Schematic



NOT TO SCALE

Appendix F: Bill of Materials

This section provides list all materials and components present in the module design.

Table 3: Bill of Materials

Category	Item	Quantity	Source
Electronics	HS-77BB Servo, Clockwise	2	Servocity.com
Hardware	24 Tooth Spline Servo to Shaft Couplers, Bore: 0.250"	2	Servocity.com
	Stainless Steel Ball Bearing Open Flanged, for 0.25" Shaft Diameter, 0.5" OD	4	McMaster Carr
	T-Nut, 0.125" ID, Fine Thread	4	Local Hardware
	Bolt, 0.125", Fine Thread, Countersunk Head, 0.75" Length	4	Local Hardware
	Carriage Bolt, 0.25" Coarse Thread, 3" Length	4	Local Hardware
	Hex Nut, 0.25", Coarse Thread	4	Local Hardware
Raw Materials	Metal Rod, 0.25" Diameter, 6061 Aluminum, 12" Length	1	Alro Metals
	Birch Plywood Sheet, 0.125" Thick, 20" Wide, 20" Long	1	Local Hardware
	Cyanoacrylate Glue, 3 Second Set Time	1	Local Hobby Store